

Cooperative Interactions in a Ternary Mixture

Adrian P. Bisson, Christopher A. Hunter,* Juan Carlos Morales, and Karen Young

Abstract: The formation of hydrogen-bonded complexes between three different compounds has been investigated by ^1H NMR spectroscopy. Titration experiments for binary and ternary mixtures show that these compounds form a termolecular complex in chloroform. The complexation-induced changes in chemical shift indicate that the structure of the ternary complex is similar to the

hydrogen-bonded structures found in the simple binary mixtures. However, the association constant for the formation of the ternary complex is significantly larger than that expected based

Keywords: amides • cooperative effects • hydrogen bonds • NMR spectroscopy

on the stabilities of the binary complexes: the association constant increases by a factor of three, equivalent to a stabilisation of $1-2 \text{ kJ mol}^{-1}$. An explanation for this phenomenon is that the formation of a small hydrogen-bond network polarises the hydrogen-bonding groups and thereby increases the strengths of the individual hydrogen-bonding interactions.

Introduction

When many weak noncovalent interactions act in concert to generate an organised structure, for example in a crystalline solid or a folded protein, the net release of free energy is often greater than one might expect based on the properties of the individual intermolecular interactions studied in isolation.^[1] This phenomenon, cooperativity, has two important origins. One noncovalent interaction can sense (and respond to) the presence of another noncovalent interaction either through a change in the number of degrees of freedom accessible to the system or through a change in the electronic structures of the molecules.

Cooperativity mediated by conformational change and restriction of conformational, translational or rotational mobility is an essential aspect of any molecular recognition event. Figures 1 and 2 distinguish two different situations in which these concepts apply. Figure 1 shows cooperativity between different interaction sites on the same molecules for these bimolecular complexes $|\Delta G_{AB}| > |\Delta G_A + \Delta G_B|$. This is often entropy-driven, but may also have an enthalpic contribution.^[2-5] Figure 2 shows cooperativity between different interaction sites on different molecules: for these termo-

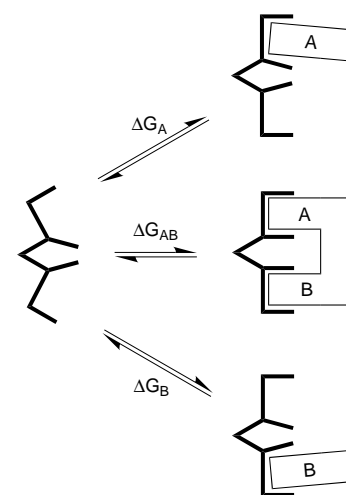


Figure 1. Cooperative binding interactions between two recognition sites on the same molecule in a bimolecular complex. Complexation of the covalently linked adduct AB is entropically more favourable than complexation of the two separate recognition elements A and B. $|\Delta G_{AB}| > |\Delta G_A + \Delta G_B|$.

lecular (or larger) complexes $|\Delta G_2| > |\Delta G_1|$. This can be due to a change in the conformation of the receptor induced by the binding of the first substrate (Figure 2a) or to direct interactions between the two substrates in the ternary complex (Figure 2b).^[6-12]

Cooperativity mediated by changes in electronic structure is a quite distinct phenomenon and is related to an important fundamental property of all noncovalent interactions, induction. In polar systems that contain intermolecular electrostatic

[*] Prof. C. A. Hunter, A. P. Bisson, K. Young, J. C. Morales
 Krebs Institute for Biomolecular Science, Department of Chemistry
 University of Sheffield, Sheffield, S3 7HF (UK)
 Fax: (+44) 114-273-8673
 E-mail: c.hunter@sheffield.ac.uk
 J. C. Morales
 Instituto de Química Organica, CSIC, Juan Cierva 3
 E-28006 Madrid (Spain)

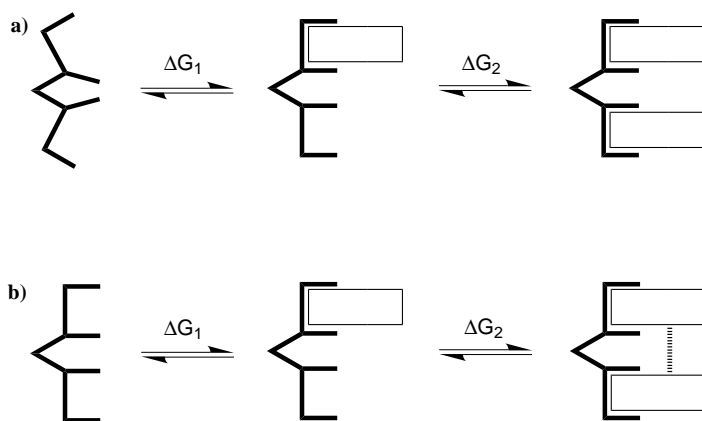


Figure 2. Cooperative binding interactions between two recognition sites on different molecules in a ternolecular complex. a) Complexation of the first substrate changes the conformation of the receptor. b) Direct interactions between the two substrates stabilise the ternary complex. In both cases $|\Delta G_2| > |\Delta G_1|$.

interactions strong enough to perturb the electronic charge distributions of the molecules, the induced polarisation causes an additional contribution to the total electrostatic interaction energy over and above what might be expected, based on the charge distributions of the isolated molecules. Such induction effects are believed to be important in protein folding, where networks of amide–amide hydrogen bonds (e.g., in α helices) are believed to reinforce each other. The formation of one amide–amide hydrogen bond increases the magnitude of the N–H and C=O bond dipoles, so that the formation of a second hydrogen bond on the other face of the amide is energetically more favourable (Figure 3).^[13] ΔG_2 in Figure 3 is

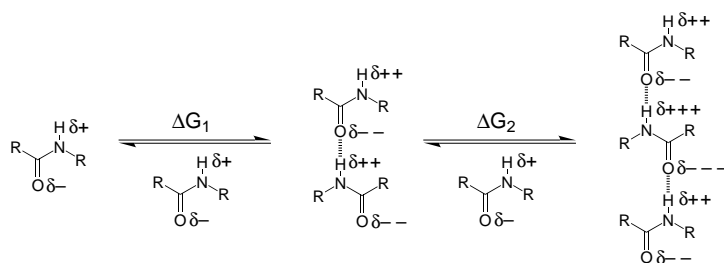


Figure 3. Cooperative binding interactions caused by induction. The formation of hydrogen bonds increases the polarisation of the amide groups, and so $|\Delta G_2| > |\Delta G_1|$.

more favourable than ΔG_1 , because the ternolecular complex involves hydrogen-bonding interactions between amides that are more highly polarised than the amides in the bimolecular complex. The difference ($\Delta G_2 - \Delta G_1$) is a measure of the magnitude of this electrostatic cooperativity. However, experimentally the magnitude of such cooperative interactions is not easy to quantify, and so evidence that such effects are energetically significant for protein folding or small molecule recognition is lacking.^[14]

Recently, Williams et al. presented experimental evidence for cooperativity in the formation of a quaternary complex of two molecules of vancomycin and two molecules of *N*-Ac-D-Ala-D-Ala.^[15] A network of hydrogen bonds is formed at the

intermolecular interface in this system, and the cooperativity could be attributed to the inductive polarisation effects illustrated in Figure 3. However, the molecules are charged and the effect might simply be a consequence of a direct electrostatic interaction between the positive charges on the vancomycins with the negative charges on the peptide substrates as in Figure 2b. In this paper, we describe an experimental study of a small molecule system that suggests that inductive cooperativity makes a significant energetic contribution to the free energy of hydrogen-bonding interactions between neutral molecules in organic solvents.

Approach: We recently described the structures of a family of amide oligomers that form dimeric hydrogen-bonded complexes in chloroform.^[16] The structure of one of these complexes (**1**·**2**) is shown in Figure 4a. This system represents

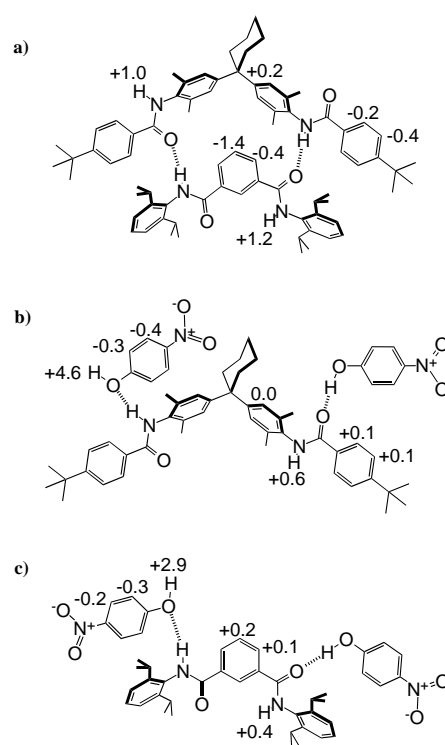
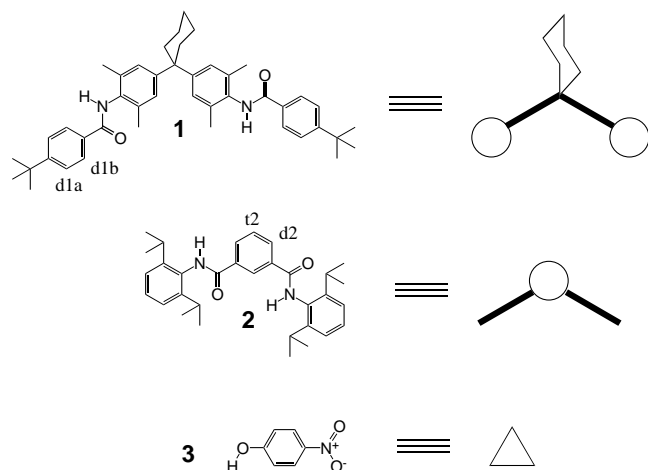


Figure 4. Structures of the complexes formed in binary mixtures of **1**, **2** and **3**. The limiting complexation-induced changes in ^1H NMR chemical shift determined by extrapolating titration data in chloroform are indicated. a) Structure of the 1:1 complex formed between **1** and **2**. b) Representative structure indicating the important interactions present in the **1**·(**3**)₂ complex. Different structures where **3** is bound on the other face of **1** are probably present in this system. c) Representative structure indicating the important interactions present in the **2**·(**3**)₂ complex. Different structures where **3** is bound on the other face of **2** are probably present in this system.

a simple model for probing various aspects of molecular recognition such as the magnitude of the individual interactions, which contribute to the stability of the complex,^[17–18] their sensitivity to substituents and the magnitude of cooperative interactions between them. Here we report an experiment designed to detect induction effects in a small hydrogen-bond network. The idea is simply to add a third component that is capable of forming hydrogen bonds with the **1**·**2**

complex and to measure consequent changes in the stability of the complex. *p*-Nitrophenol (**3**) was chosen as the third component (Scheme 1), since it is a good hydrogen-bond donor and additional π – π interactions should stabilise the complexes sufficiently for accurate determination of association constants.



Scheme 1. The structures of **1**, **2** and **3** with the ^1H NMR signal labelling scheme.

Results and Discussion

Binary mixtures: We first investigated the properties of the three possible two component mixtures of **1**, **2** and **3**. The **1**·**2** complex has already been described, but the key results are repeated here for comparison with the ternary mixtures.^[17] The complexes were characterised in deuteriochloroform by means of ^1H NMR Job plots to determine the stoichiometries (Figure 5) and ^1H NMR titrations to determine the association constants (Table 1) and complexation-induced changes in chemical shift (Figure 4). The Job plots show that **1** and **2** form a 1:1 complex as described previously, but the results for the other two complexes are not so simple. For both systems, the Job plots show some asymmetry which means that the stoichiometry is greater than 1:1. The simplest interpretation is that these systems form 2:1 complexes, but that the two binding sites are slightly different: they may have different complexation-induced changes in chemical shift or different association constants that displace the maximum in the Job plot from 0.67 (or 0.33). The titration data for the complexes containing **3** were analysed with curve-fitting software and various different binding models: 1:1 complexation, 2:1 complexation with identical binding sites and 2:1 complexation with different binding sites. In fact, the results were rather similar for all of these models, and we conclude that the difference between the two binding sites is small.

All three titrations were performed firstly with one binding partner as the host and they were then repeated with the other binding partner as the host, so that reliable complexation-induced changes in ^1H NMR chemical shift could be determined for both molecules in the complex (Figure 4). These changes in chemical shift give an indication of the

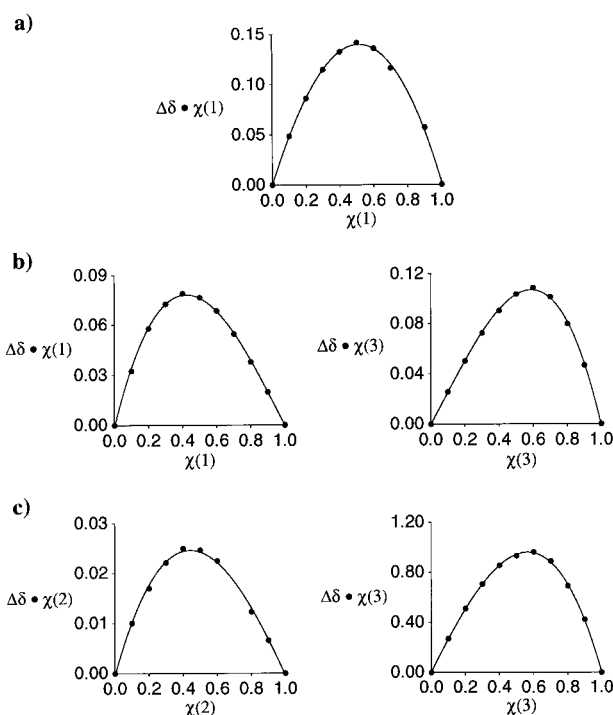


Figure 5. ^1H NMR Job plots for the binary mixtures of **1**, **2** and **3** in chloroform: a) **1** + **2**. b) **1** + **3**. c) **2** + **3**.

Table 1. Association constants in chloroform at 295 K.^[a]

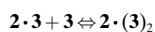
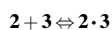
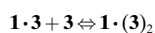
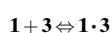
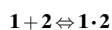
	K_1 [M^{-1}]	K_2 [M^{-1}]	$K(\mathbf{1}\cdot\mathbf{2}\cdot\mathbf{3})$ [M^{-2}]
$\mathbf{1} + \mathbf{2} \rightleftharpoons \mathbf{1}\cdot\mathbf{2}$	47 ± 3	–	–
$\mathbf{1} + \mathbf{3} \rightleftharpoons \mathbf{1}\cdot\mathbf{3} + \mathbf{1}\cdot(\mathbf{3})_2$	52 ± 5	51 ± 5	–
$\mathbf{2} + \mathbf{3} \rightleftharpoons \mathbf{2}\cdot\mathbf{3} + \mathbf{2}\cdot(\mathbf{3})_2$	21 ± 3	22 ± 3	–
$\mathbf{1}\cdot\mathbf{2} + \mathbf{3} \rightleftharpoons \mathbf{1}\cdot\mathbf{2}\cdot\mathbf{3}$	240 ± 50	–	$11\,000 \pm 3000$
$\mathbf{1}\cdot\mathbf{3} + \mathbf{2} \rightleftharpoons \mathbf{1}\cdot\mathbf{2}\cdot\mathbf{3}$	150 ± 50	–	8000 ± 3000
$\mathbf{2}\cdot\mathbf{3} + \mathbf{1} \rightleftharpoons \mathbf{1}\cdot\mathbf{2}\cdot\mathbf{3}$	270 ± 80	–	6000 ± 2000

[a] Average values from at least two separate experiments. Titration data for three–six different signals were used to determine the association constant in each experiment. Errors are quoted as twice the standard error from the weighted mean (weighting based on the observed change in chemical shift).

structures of these complexes (protons for which changes in chemical shift are not shown in Figure 4 moved less than 0.15 ppm in all of the complexes). Downfield shifts of the amide and hydroxyl protons are characteristic of hydrogen-bonding interactions, while upfield shifts of the aromatic protons are indicative of π – π interactions. The structure of the **1**·**2** complex with two hydrogen bonds and four edge-to-face π – π interactions is shown in Figure 4a. Representative structures for the complexes formed with **3** are shown in Figures 4b and c: the changes in chemical shift indicate hydrogen bonds between the amides of **1** and **2** and the hydroxyl group of **3**, and the upfield shifts of the signals due to the aromatic protons of **3** are characteristic of edge-to-face π – π interactions. Although a mixture of conformations is probably present in these systems, the very large shifts observed for the **3** hydroxyl proton suggest that the primary mode of interaction involves H-bonds, where the **3** hydroxyl proton is the donor and the amide oxygens of **1** and **2** are the acceptors. This observation is also consistent with the

formation of 2:1 complexes where each amide carbonyl oxygen of **1** and **2** forms a hydrogen bond to a molecule of **3**.

Ternary mixture: The ternary mixture was studied by means of ^1H NMR titrations.^[19] One component was titrated into a 1:1 mixture of the other two components in deuteriochloroform. In principle, the ternary mixture might contain no new equilibria, and so the binding isotherms obtained from these titrations could be predicted from the known binding constants and complexation-induced changes in chemical shift from the binary mixture experiments. We therefore used simulation software to calculate the binding isotherms for the ternary mixture titrations with a model that simultaneously accounted for all of the equilibria (a)–(e) and the known properties of the binary mixtures.



The results of these simulations along with the experimental data for the titration of **3** into a 1:1 mixture of **1** and **2** are shown in Figure 6 (see also Scheme 1). There is a large difference between the simulated binding isotherms and the experimental data. Notably, the signals due to four of the aromatic protons all show biphasic behaviour that can not be explained by the binary equilibria (Figures 6a–d). This shows that there is at least one additional species present in the ternary mixture that is not present in any of the binary mixtures. The only explanation is a complex that contains all three components, **1**, **2** and **3**. Figure 7 shows the equilibria that are present. At the start of the titration, in the presence of small amounts of **3**, the ternary complex is formed, but as the titration proceeds the excess **3** forces the equilibrium towards the binary mixture complexes. This explains the biphasic nature of the titration data in Figure 6: the decrease in the chemical shifts of the signals due to the **1** and **2** aromatic protons is a result of the formation of the ternary complex, and the increase in chemical shift in the second phase of the titration corresponds to dissociation of this complex and formation of the simple binary mixture complexes. The signals due to the four aromatic protons in Figure 6 are precisely the four signals that show large upfield shifts on formation of the **1**·**2** complex: indeed the magnitude of the downward curvature in Figure 6 closely matches the size of the complexation-induced change in chemical shift in the **1**·**2** complex. This observation suggests that the structure of the ternary complex is very similar to that of the **1**·**2** complex. The large increase in the chemical shifts of the signals due to the amide protons over and above that expected for the simple binary mixture complexes suggests that the ternary complex involves additional hy-

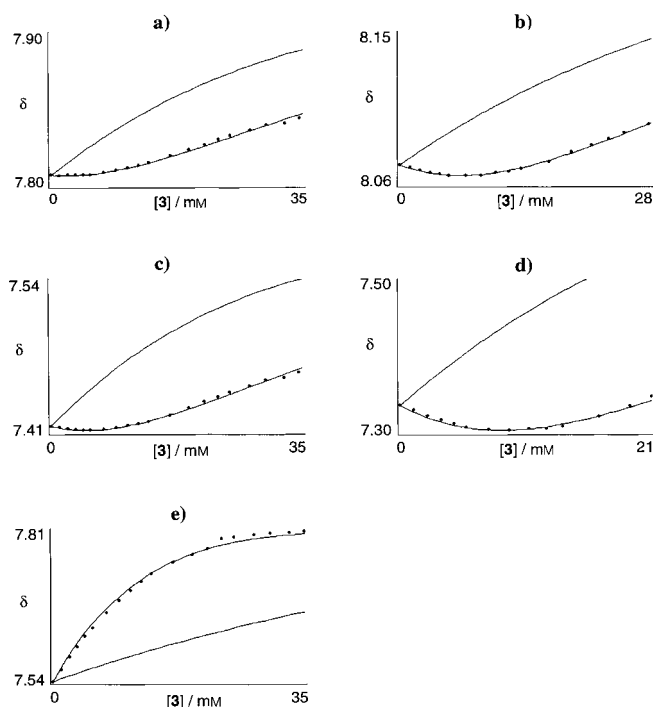


Figure 6. ^1H NMR titration data for the addition of **3** to a 1:1 mixture of **1** and **2** in chloroform. The curves that do not fit the data points represent the predicted isotherms based on the properties of the binary mixtures. The curves that fit the data points well were obtained by including one additional equilibrium (formation of the **1**·**2**·**3** complex) in the analysis. For comparison, the changes in chemical shift ($\Delta\delta$) in the **1**·**2** complex are given. a) signal d1b, $\Delta\delta$ in **1**·**2** complex = -0.2 . b) signal d2, $\Delta\delta$ in **1**·**2** complex = -0.4 . c) signal d1a, $\Delta\delta$ in **1**·**2** complex = -0.4 . d) signal t2, $\Delta\delta$ in **1**·**2** complex = -1.4 . e) signal NH1, $\Delta\delta$ in **1**·**2** complex = $+1.0$. The signal labelling scheme is shown on the structure diagrams in Scheme 1.

drogen-bonding interactions (Figure 6e). In conclusion, the structure of the ternary complex is essentially identical to that of the **1**·**2** complex with a molecule of **3** hydrogen bonded on the outside, shown schematically in Figure 7. One of the possible structures consistent with these observations is shown in Figure 8.^[20]

In order to obtain an estimate of the stability of the ternary complex, the experimental data was analysed with curve-fitting software with a model that accounted for all of the

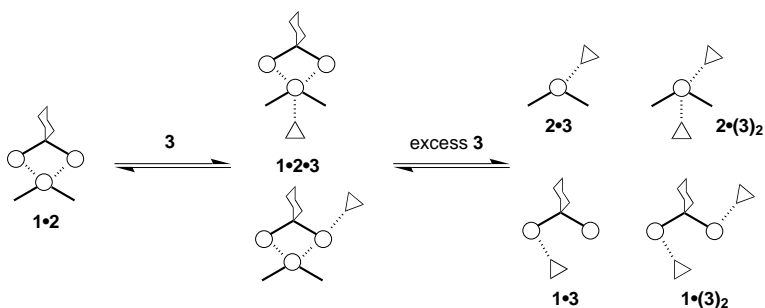


Figure 7. Schematic representation of the complexes present in the ternary mixture. Following the equilibria from left to right illustrates the progress of the titration of **3** into a 1:1 mixture of **1** and **2**. Initially, the **1**·**2** complex is present. As **3** is added, the ternary complex, **1**·**2**·**3**, is formed. On addition of excess **3**, this complex is broken up and a mixture of **1**·**3** and **2**·**3** complexes are formed.

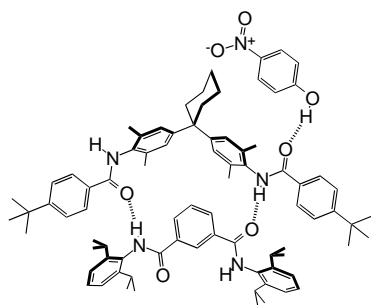
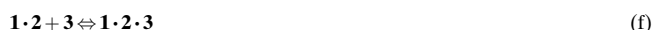


Figure 8. Structure of the ternary complex, **1·2·3**. Other binding modes where **3** is hydrogen-bonded to different amide groups on the outside of the **1·2** complex are also populated.

binary equilibria (a)–(e) and an additional equilibrium (f)–(h) for the formation the ternary complex **1·2·3**. When **3** was



titrated into the 1:1 mixture of **1** and **2** equilibrium (f) was included in the analysis, when **1** was titrated into the 1:1 mixture of **2** and **3** equilibrium (g) was included and when **2** was titrated into the 1:1 mixture of **1** and **3** equilibrium (h) was included.

The results discussed above show that the structure of the ternary complex is similar to that of the **1·2** complex with **3** bound on the outside (Figure 7). We therefore used this model to estimate the bound chemical shift of the ternary complex. This allows us to carry out the curve-fitting with a single variable, the association constant for formation of the ternary complex, which significantly improves the reliability of the fitting procedure. Five different values for the bound chemical shift of the ternary complex that correspond to different possible binding modes were tested as detailed in Equations (1)–(5).

$$\Delta\delta(\mathbf{1} \cdot \mathbf{2} \cdot \mathbf{3}) = \Delta\delta(\mathbf{1} \cdot \mathbf{2}) \quad (1)$$

$$\Delta\delta(\mathbf{1} \cdot \mathbf{2} \cdot \mathbf{3}) = \Delta\delta(\mathbf{1} \cdot \mathbf{2}) + \Delta\delta(\mathbf{1} \cdot \mathbf{3}) \quad (2)$$

$$\Delta\delta(\mathbf{1} \cdot \mathbf{2} \cdot \mathbf{3}) = \Delta\delta(\mathbf{1} \cdot \mathbf{2}) + \Delta\delta(\mathbf{2} \cdot \mathbf{3}) \quad (3)$$

$$\Delta\delta(\mathbf{1} \cdot \mathbf{2} \cdot \mathbf{3}) = \Delta\delta(\mathbf{1} \cdot \mathbf{2}) + \Delta\delta(\mathbf{1} \cdot \mathbf{3}) + \Delta\delta(\mathbf{2} \cdot \mathbf{3}) \quad (4)$$

$$\Delta\delta(\mathbf{1} \cdot \mathbf{2} \cdot \mathbf{3}) = \Delta\delta(\mathbf{1} \cdot \mathbf{2}) + 0.5\{\Delta\delta(\mathbf{1} \cdot \mathbf{3}) + \Delta\delta(\mathbf{2} \cdot \mathbf{3})\} \quad (5)$$

The results obtained were very similar for all of these models for all three titrations: the change in chemical shift for formation of the **1·2** complex is generally much larger than for the other complexes, and so the difference between different models is small. The quality of the fit of the calculated curve to the experimental data for such a complex system with a single variable, the ternary complex association constant, is remarkably good (Figure 6), especially since it is usually difficult to obtain good curve fits with biphasic isotherms. The association constants for each of the three titrations are listed in Table 1 (these figures and the fits shown

in Figure 6 were obtained from the last method for estimating $\Delta\delta(\mathbf{1} \cdot \mathbf{2} \cdot \mathbf{3})$ shown above [Eq. (5)]). All three titrations show substantial increases in the observed association constant (K_1) compared with the binary mixture complexes; this indicates that some kind of cooperative interactions are present in the ternary complex. The K_1 values in Table 1 are the association constants for the formation of **1·2·3** from the corresponding binary complex. The value for the association constant for formation of the ternary complex from the three constituent molecules, $K(\mathbf{1} \cdot \mathbf{2} \cdot \mathbf{3})$, is determined by combining the appropriate equilibrium constants as follows:

$$\text{For titration } \mathbf{1} \cdot \mathbf{2} + \mathbf{3} \rightleftharpoons \mathbf{1} \cdot \mathbf{2} \cdot \mathbf{3} \quad K(\mathbf{1} \cdot \mathbf{2} \cdot \mathbf{3}) = K_1(\text{obs})K_1(\mathbf{1} \cdot \mathbf{2})$$

$$\text{For titration } \mathbf{2} \cdot \mathbf{3} + \mathbf{1} \rightleftharpoons \mathbf{1} \cdot \mathbf{2} \cdot \mathbf{3} \quad K(\mathbf{1} \cdot \mathbf{2} \cdot \mathbf{3}) = K_1(\text{obs})K_1(\mathbf{2} \cdot \mathbf{3})$$

$$\text{For titration } \mathbf{1} \cdot \mathbf{3} + \mathbf{2} \rightleftharpoons \mathbf{1} \cdot \mathbf{2} \cdot \mathbf{3} \quad K(\mathbf{1} \cdot \mathbf{2} \cdot \mathbf{3}) = K_1(\text{obs})K_1(\mathbf{1} \cdot \mathbf{3})$$

The value of $K(\mathbf{1} \cdot \mathbf{2} \cdot \mathbf{3})$ shows some variation between the three titrations, but the results fall within the range of the estimated errors: the average value is $8000 \pm 2000 \text{ M}^{-2}$. The magnitude of the cooperativity observed in the ternary complex can thus be determined by comparing this association constant with the individual bimolecular association constants. The two most stable bimolecular complexes are **1·2** and **1·3**, and therefore these make the most appropriate comparison.

$$\text{Cooperativity factor} = \frac{K(\mathbf{1} \cdot \mathbf{2} \cdot \mathbf{3})}{K(\mathbf{1} \cdot \mathbf{2})K(\mathbf{1} \cdot \mathbf{3})} = 3$$

In other words, cooperative interactions in the ternary complex make it three times more stable than expected, based on the strengths of the individual interactions in the two bimolecular complexes. This stabilisation is equivalent to $1-2 \text{ kJ mol}^{-1}$, and we attribute the additional interaction energy to induction effects caused by polarisation of the amides and enhanced hydrogen-bonding interactions in the ternary complex as illustrated in Figure 3.

It is not possible to obtain more detailed information on the structure of the ternary complex, for example from ROESY experiments, because the proportion of this complex present is always small. Figure 9 shows how the populations of the

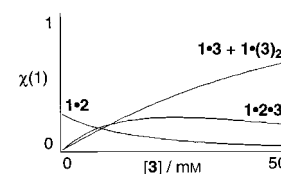


Figure 9. Populations of complexes present during the titration of **3** into a 1:1 mixture of **1** and **2**.

various species change during the course of the titration of **3** into the 1:1 mixture of **1** and **2**. The concentration of the ternary complex goes through a maximum at about 25 mM, and it is only ever present as 25% of the total concentration of **1** (or **2**). There is always a comparable amount of the **1·3** complex present, so that it is difficult to obtain useful unambiguous structural information from the ROESY spectrum of the mixture.

Conclusions

These experiments show that **1**, **2** and **3** form a termolecular complex in chloroform solution. The complexation-induced changes in chemical shift indicate that the structure of the ternary complex is similar to the hydrogen-bonded structures found in the simple binary mixtures. However, the association constant for formation of the ternary complex is significantly larger than that expected based on the stabilities of the binary complexes (the increase of a factor of three is equivalent to 1–2 kJ mol⁻¹). This enhanced stability might be explained by a conformational change or by direct interactions between all three molecules in the ternary complex, but the most likely explanation is that the formation of a small hydrogen-bond network polarises the hydrogen-bonding groups and thereby increases the strengths of the individual hydrogen-bonding interactions. This result shows that induction effects can be important even at the level of simple small molecule interactions where two hydrogen bonds can mutually stabilise each other by perturbing the molecular charge distributions. These experiments have been carried out in chloroform, which is a very weak hydrogen-bonding solvent. It is not clear that the results will also apply to molecular recognition in water where all of the functional groups would be strongly hydrogen-bonded to the solvent at all times.

Experimental Section

p-Nitrophenol (**3**) was purchased from Aldrich and used without further purification. Compounds **1** and **2** were prepared by simple amide couplings as outlined below.

Synthesis of 1: *p*-tert-Butyl benzoyl chloride (8.4 mmol; 1.6 mL) was added to a solution of 1,1'-bis(4-amino-3,5-dimethylphenyl)cyclohexane^[21] (4.2 mmol; 1.35 g) and Et₃N (8.4 mmol; 1.2 mL) in dry CH₂Cl₂ (50 mL) over 10 min. The reaction was allowed to stir for two hours. The solution was washed with HCl (1M; 2 × 75 mL) and NaOH (1M; 2 × 75 mL) and then dried over Na₂SO₄ (anhydrous). The Na₂SO₄ was removed by filtration and the organic solution reduced to dryness on the rotary evaporator. The product was isolated by recrystallization from CH₂Cl₂/petroleum ether (40–60) to give a clear yellow solid (2.5 g; 92%). M.p. 192–193 °C; ¹H NMR (250 MHz, CDCl₃, 25 °C, TMS): δ = 7.84 (d, ³J(H,H) = 7 Hz, 4H), 7.52 (d, ³J(H,H) = 7 Hz, 4H), 7.27 (s, 2H), 7.03 (s, 4H), 2.24 (m, 16H), 1.60–1.45 (m, 6H), 1.55 (s, 18H); ¹³C NMR (250 MHz, [D₆]DMSO, 25 °C): δ = 165.2, 154.5, 147.0, 135.5, 133.1, 132.0, 127.8, 126.3, 125.5, 45.1, 36.5, 35.0, 31.3, 26.2, 23.1, 18.9; IR (C₂H₂Cl₄): $\tilde{\nu}$ = 3425, 2980, 2968, 2865, 1669, 1610, 1565, 1489, 1365 cm⁻¹; MS (FAB): *m/z* (%): 642 [*M*⁺]; C₄₄H₅₄N₂O₂ (642): calcd C 82.20, H 8.47, N 4.36; found C 82.17, H 8.46, N 4.20.

Synthesis of 2: 2,6-Diisopropyl aniline (0.011 mol; 2.2 mL) and Et₃N (0.0118 mol; 1.6 mL) in dry CH₂Cl₂ (25 mL) were added to a solution of isophthaloyl dichloride (5.9 mmol; 1.2 g) in dry CH₂Cl₂ (50 mL). The reaction was allowed to stir for two hours and then diluted to 150 mL with CH₂Cl₂. The reaction mixture was washed with HCl (1M; 2 × 100 mL) and NaOH (1M; 2 × 100 mL), and the resultant organic solution dried over Na₂SO₄ (anhydrous). The Na₂SO₄ was removed by filtration and the organic solution reduced to dryness on a rotary evaporator. The resultant cream solid was recrystallized from CH₂Cl₂/petroleum ether (40–60) to give the product as a white solid (2.7 g; 95%). M.p. >270 °C; ¹H NMR (250 MHz, CDCl₃, 25 °C, TMS): δ = 8.52 (s, 1H), 8.10 (d, ³J(H,H) = 7 Hz, 2H), 7.60 (m, 3H), 7.35 (t, ³J(H,H) = 7 Hz, 1H), 7.23 (d, ³J(H,H) = 7 Hz,

4H), 3.15 (septet, ³J(H,H) = 7 Hz, 2H), 1.25 (d, ³J(H,H) = 7 Hz, 24H); ¹³C NMR (250 MHz, [D₆]DMSO, 25 °C): δ = 166.2, 149.8, 146.5, 135.2, 133.0, 130.0, 128.0, 127.5, 123.4, 28.7, 24.0, 23.8; IR (C₂H₂Cl₄): $\tilde{\nu}$ = 3423, 2999, 2968, 2871, 1723, 1675, 1585, 1493, 1470 cm⁻¹; MS (FAB): *m/z* (%): 485 [*MH*⁺]; C₃₃H₄₀N₂O₂ (484): calcd C 79.30, H 8.32, N 5.78; found C 79.03, H 8.24, N 5.48.

¹H NMR Titrations: A sample of host was dissolved in deuteriochloroform (generally concentrations of 5–20 mM were used). A portion of this solution was used as the host NMR sample, and the remainder was used to dissolve a sample of the guest, so that the host concentration remained constant throughout the titration. Successive aliquots of the guest solution were added to the host NMR sample, and ¹H NMR spectra were recorded after each addition. The changes in chemical shift of all of the host signals as a function of guest concentration were then analysed with purpose-written software on an Apple Macintosh microcomputer. These programmes fit the data to the appropriate binding model to yield the association constant, the bound chemical shift and, if required, the free chemical shift.

NMRTit HG fits the data to a 1:1 binding isotherm by solving the Equations (6)–(8) in which [H]₀ is the total concentration of host; [G]₀ is the total concentration of guest; [H] is the concentration of unbound free host; [HG] is the concentration of host·guest complex; *K* is the association constant for formation of the host·guest complex; δ_f is the free chemical shift of the host; δ_b is the limiting bound chemical shift of the host·guest complex.

$$[\text{HG}] = \frac{1 + K[\text{H}]_0[\text{G}]_0 - \sqrt{\{(1 + [\text{H}]_0[\text{G}]_0)^2 - 4K^2[\text{H}]_0[\text{G}]_0\}}}{2K} \quad (6)$$

$$[\text{H}] = [\text{H}]_0 - [\text{HG}] \quad (7)$$

$$\delta_{\text{obs}} = \frac{[\text{HG}]}{[\text{H}]_0} \delta_{\text{b}} + \frac{[\text{H}]}{[\text{H}]_0} \delta_{\text{f}} \quad (8)$$

NMRTit HGG fits the data to a 1:2 binding isotherm by an iterative procedure to solve the following simultaneous equations. The method starts by assuming that [HGG] = 0, so that Equation (9) can be solved exactly for [HG]. This value of [HG] is then used to solve Equation (10) for [HGG]. Equation (11) gives the concentration of free host [H]. At this point, [H] + [HG] + [HGG] = [H]₀, so the value of [HGG] from Equation (10) is used in Equation (9) to reevaluate [HG], and the procedure is carried out repetitively until [H] + [HG] + [HGG] = [H]₀. This allows the set of simultaneous equations [Eq. (9)–(12)] to be solved for the concentrations of all species present where [HG] is the concentration of host·(guest)₂ complex; *K*₁ is the microscopic association constant for formation of the host·guest complex; *K*₂ is the microscopic association constant for

$$[\text{HG}] = \frac{1 + 2K_1[\text{G}]_0([\text{H}]_0 - [\text{HGG}]) - \sqrt{\{(1 + 2K_1[\text{G}]_0([\text{H}]_0 - [\text{HGG}])\}^2 - 16K_1^2[\text{G}]_0([\text{H}]_0 - [\text{HGG}])\}}}{4K_1} \quad (9)$$

$$[\text{HGG}] = \frac{1 + 0.5K_2[\text{G}]_0([\text{H}]_0 - [\text{HG}]) - \sqrt{\{(1 + 0.5K_2[\text{G}]_0([\text{H}]_0 - [\text{HG}])\}^2 - K_2[\text{G}]_0([\text{H}]_0 - [\text{HG}])\}}}{K_2} \quad (10)$$

$$[\text{H}] = [\text{H}]_0 - [\text{HG}] - [\text{HGG}] \quad (11)$$

$$\delta_{\text{obs}} = \frac{[\text{HGG}]}{[\text{H}]_0} \delta_{\text{b2}} + \frac{[\text{HG}]}{[\text{H}]_0} \delta_{\text{b1}} + \frac{[\text{H}]}{[\text{H}]_0} \delta_{\text{f}} \quad (12)$$

formation of the host·(guest)₂ complex; δ_{b1} is the limiting bound chemical shift of the host·guest complex; δ_{b2} is the limiting bound chemical shift of the host·(guest)₂ complex.

NMRTit HHG fits the data to a 2:1 binding isotherm by an iterative procedure to solve the following simultaneous equations. The method is similar to that described above for *NMRTit HGG*. The procedure starts by assuming that [HHG] = 0, and then Equations (13)–(16) are solved in turn repetitively until [H] + [HG] + 2[HHG] = [H]₀, where [HHG] is the concentration of (host)₂·guest complex; *K*₁ is the microscopic association constant for formation of the host·guest complex; *K*₂ is the microscopic

$$[\text{HG}] = \frac{1 + 2K_1[\text{G}]_0([\text{H}]_0 - 2[\text{HHG}]) - \sqrt{\{(1 + 2K_1[\text{G}]_0([\text{H}]_0 - 2[\text{HHG}])\}^2 - 16K_1^2[\text{G}]_0([\text{H}]_0 - 2[\text{HHG}])\}}}{4K_1} \quad (13)$$

$$[\text{HHG}] = \frac{1 + 0.5K_2[\text{G}]_0([\text{H}]_0 - [\text{HG}]) - \sqrt{\{(1 + 0.5K_2[\text{G}]_0([\text{H}]_0 - [\text{HG}])\}^2 - K_2^2[\text{G}]_0([\text{H}]_0 - [\text{HG}])\}}}{K_2} \quad (14)$$

$$[\text{H}] = [\text{H}]_0 - [\text{HG}] - 2[\text{HHG}] \quad (15)$$

$$\delta_{\text{obs}} = \frac{2[\text{HHG}]}{[\text{H}]_0} \delta_{\text{b2}} + \frac{[\text{HG}]}{[\text{H}]_0} \delta_{\text{b1}} + \frac{[\text{H}]}{[\text{H}]_0} \delta_{\text{f}} \quad (16)$$

association constant for formation of the (host)₂·guest complex; δ_{b1} is the limiting bound chemical shift of the host·guest complex; δ_{b2} is the limiting bound chemical shift of the (host)₂·guest complex.

The approach for the multiple equilibria in the ternary mixture is the same, and the programmes use the same iterative procedure to solve the appropriate set of simultaneous equations. These curve fitting programmes are available from the author on request. All experiments were performed at least twice. The association constant for a single run was calculated as the mean of the values obtained for each of the signals followed during the titration, weighted by the observed changes in chemical shift. The association constants from different runs were then averaged. Errors are quoted at the 95% confidence limits (twice the standard error). For a single run, the standard error was determined from the standard deviation of the different association constants determined by following different signals.

Acknowledgements: We thank the EPSRC (A.P.B.), the University of Sheffield (K.Y.), the Spanish government (J.C.M.) and the Lister Institute (C.A.H.) for financial support.

Received: October 27, 1997 [F864]

- [1] M. S. Westwell, M. S. Searle, D. H. Williams, *J. Mol. Rec.* **1996**, *9*, 88–94.
- [2] A. Pfeil, J. M. Lehn, *J. Chem. Soc. Chem. Commun.* **1992**, 838–840.
- [3] P. Groves, M. S. Searle, M. S. Westwell, D. H. Williams, *J. Chem. Soc. Chem. Commun.* **1994**, 1519–1520.
- [4] M. S. Searle, G. J. Sharman, P. Groves, B. Benhamu, D. A. Beauregard, M. S. Westwell, R. J. Dancer, A. J. Maguire, A. C. Try, D. H. Williams, *J. Chem. Soc. Perkin Trans. 1* **1996**, 2781–2786.
- [5] A. P. Bisson, C. A. Hunter, *Chem. Commun.* **1996**, 1723–1724.
- [6] K. Onan, J. Rebeck, T. Costello, L. Marshall, *J. Am. Chem. Soc.* **1983**, *105*, 6759–6760.
- [7] C. A. Hunter, D. H. Purvis, *Angew. Chem.* **1992**, *104*, 779; *Angew. Chem. Int. Ed. Engl.* **1992**, *31*, 792–795.
- [8] D. A. Bell, S. G. Diaz, V. M. Lynch, E. V. Anslyn, *Tet. Lett.* **1995**, *36*, 4155–4158.
- [9] J. S. Lindsey, *New J. Chem.* **1991**, *15*, 153–180.
- [10] M. D. Distefano, P. B. Dervan, *Proc. Natl. Acad. Sci. USA* **1993**, *90*, 1179–1183.
- [11] N. Colocci, M. D. Distefano, P. B. Dervan, *J. Am. Chem. Soc.* **1993**, *115*, 4468–4473.
- [12] N. Colocci, P. B. Dervan, *J. Am. Chem. Soc.* **1995**, *117*, 4781–4787.
- [13] H. Guo, M. Karplus, *J. Phys. Chem.* **1994**, *98*, 7104–7105.
- [14] G. J. Sharman, M. S. Searle, *Chem. Commun.* **1997**, 1955–1956.
- [15] J. P. Mackay, U. Gerhard, D. A. Beauregard, M. S. Westwell, M. S. Searle, D. H. Williams, *J. Am. Chem. Soc.* **1994**, *116*, 4581–4590.
- [16] A. P. Bisson, F. J. Carver, C. A. Hunter, J. P. Waltho, *J. Am. Chem. Soc.* **1994**, *116*, 10292–10293.
- [17] H. Adams, F. J. Carver, C. A. Hunter, J. C. Morales, E. M. Seward, *Angew. Chem.* **1996**, *108*, 1628–1631; *Angew. Chem. Int. Ed. Engl.* **1996**, *35*, 1542–1544.
- [18] H. Adams, K. D. M. Harris, G. A. Hembury, C. A. Hunter, D. Livingstone, J. F. McCabe, *Chem. Commun.* **1996**, 2531–2532.
- [19] C. S. Wilcox, J. C. Adrian, T. H. Webb, F. J. Zawacki, *J. Am. Chem. Soc.* **1992**, *114*, 10189–10197.
- [20] We assume that only one additional complex is present in the ternary mixture. Given the results obtained for the binary mixtures, we would expect more than one molecule of **3** to bind to the outside of the **1·2** complex. However, the titration data shows that there is never more than 25% of the ternary complex present. The equilibrium constant for binding of **3** to the ternary complex **1·2·3** is likely to be similar to that for binding of **3** to the **1·2** complex (240 M⁻¹), and so the proportion of tetramolecular complex **1·2·(3)₂** present at a concentration of 10⁻³ M (6%) is unlikely to be sufficient to significantly affect the analysis.
- [21] C. A. Hunter, *J. Am. Chem. Soc.* **1992**, *114*, 5303–5311.